References and Notes

1. C. L. Parkinson, D. J. Cavalieri, P. Gloersen, H. J. Zwally, J. C. Comiso. *J. Geophys. Res.* **104**, 20837 (1999).
2. K. Y. Vinnikov *et al.*, *Science* **286**, 1934 (1999).
3. M. C. Serreze *et al.*, *Clim. Change* **46**, 159 (2000).
4. D. G. Groves, J. A. Francis, *J. Geophys. Res.* **107**, 10.1029/2002JD002285 (2002).
5. W. L. Chapman, J. E. Walsh, *Bull. Am. Meteorol. Soc.* **74**, 33 (1993).
6. R. B. Myneni, C. D. Keeling, C. J. Tucker, G. Asrar, R. R. Nemani, *Nature* **386**, 698 (1997).
7. W. Meier, J. A. Maslanik, J. R. Key, C. W. Fowler, *Earth Interactions* **1** (no. 5), 1) (1997); available online at http://earthinteractions.org.
8. J. Key, "The cloud and surface parameter retrieval (CASPR) system for polar AVHRR" (Cooperative Institute for Meteorological Satellite Studies, University of Wisconsin, Madison, 2002). Available at http://stratus.ssec.wisc.edu/caspr/.
9. R. Kistler *et al.*, *Bull. Am. Meteorol. Soc.* **82**, 247 (2001).
10. W. B. Rossow, A. Walker, D. Beuschel, M. Roiter, "International Satellite Cloud Climatology Project (ISCCP) Documentation of Cloud Data" (World Climate Research Programme, NASA, Goddard Institute of Space Studies, 1996).
11. J. R. Key, X. Wang, J. Stroeve, C. Fowler, *J. Geophys. Res.* **106**, 12489 (2001).
12. J. A. Maslanik, J. R. Key, C. W. Fowler, T. Nguyen, X. Wang, *J. Geophys. Res.* **106**, 15233 (2001).
13. J. Stroeve, J. Box, C. Fowler, T. Haran, J. Key, *Remote Sens. Environ.*, **75**, 360 (2001).
14. For details on algorithm uncertainties, see Supporting Text 1.
15. I. V. Polyakov *et al.*, *J. Clim.*, in press (2002). Data are available at www.frontier.iarc.uaf.edu/~igor/data/airtemppres.php.
16. J. E. Overland, W. Muyin, N. A. Bond, *J. Clim.* **15**, 1702 (2002).
17. For a discussion of calibration uncertainties, see Supporting Text 2.
18. D. W. J. Thompson, J. M. Wallace, *Geophys. Res. Lett.* **25**, 1297 (1998).
19. Supported by the National Oceanic and Atmospheric Administration and the National Science Foundation. We thank C. Fowler, J. Maslanik, T. Scambos, and T. Haran for their work on the AVHRR Polar Pathfinder data set.

Timing of Atmospheric CO_2 and Antarctic Temperature Changes Across Termination III

Nicolas Caillon,[1,2]* Jeffrey P. Severinghaus,[2] Jean Jouzel,[1] Jean-Marc Barnola,[3] Jiancheng Kang,[4] Volodya Y. Lipenkov[5]

The analysis of air bubbles from ice cores has yielded a precise record of atmospheric greenhouse gas concentrations, but the timing of changes in these gases with respect to temperature is not accurately known because of uncertainty in the gas age–ice age difference. We have measured the isotopic composition of argon in air bubbles in the Vostok core during Termination III (~240,000 years before the present). This record most likely reflects the temperature and accumulation change, although the mechanism remains unclear. The sequence of events during Termination III suggests that the CO_2 increase lagged Antarctic deglacial warming by 800 ± 200 years and preceded the Northern Hemisphere deglaciation.

Ice cores are unique archives of past climatic and environmental conditions that provide detailed records of local temperature and atmospheric concentrations of greenhouse gases. Analyses of the Vostok ice core in Antarctica (*1*) show that concentrations of carbon dioxide correlate well with Antarctic temperature throughout the last four climatic cycles, with glacial-interglacial CO_2 increases of 80 to 100 parts per million by volume (ppmv) (*1–4*). Determining the mechanisms that cause these variations is important for understanding climate change, but the explanation for the strong link between atmospheric CO_2

and Antarctic air temperature is still unclear (*5*). One reason for this uncertainty is that the relative timing of temperature and CO_2 changes is not accurately known (*6*). The temporal relation between these two quantities is difficult to discern because air is trapped in ice at the base of the firn layer (*7*), where, at low accumulation sites such as Vostok, ice may be 6000 years old. The gas age–ice age difference (Δage) may be uncertain by 1000 years or more (*1*) and thus obscures the phasing of gas variations with climate signals borne by the ice. Although Δage and the associated uncertainty are lower at other sites where CO_2 deglacial records are available (*8*, *9*), we do not yet have a clear answer about the timing of CO_2 and Antarctic temperature changes during Terminations.

One way to circumvent this difficulty is to use records of atmospheric CO_2 content and temperature contained only in the trapped gases. During firnification, air composition is slightly modified by physical processes such as gravitational and thermal fractionation. As a result of this latter process, detectable anomalies in nitrogen and argon isotopic composition ($\delta^{15}N$ and $\delta^{40}Ar$) develop during episodes of

rapid climatic changes such as those recorded in Greenland ice cores (*10–14*). Even though we expected that thermal anomalies would be hardly detectable in the Vostok core (*15*), we searched with $\delta^{40}Ar$ measurements for a thermal signal at the start of a Termination. Given the quality and the availability of the Vostok ice, we focused first on Termination III, dated at 240,000 years before present. We observed a $\delta^{40}Ar$ change across this Termination that is closely correlated with the deuterium temperature record (*16*). This change appears to result mostly from gravitational fractionation in response to a change in the diffusive column height (DCH) (*17*), although recent model results suggest that it can be partly due to thermal fractionation (*18*). Although we do not yet clearly understand the underlying mechanisms, we argue that the $\delta^{40}Ar$ record can be taken as a climate proxy, thus providing constraints about the timing of CO_2 and climate change during Termination III.

All $\delta^{40}Ar$ measurements have been performed at the Scripps Institution of Oceanography following a wet extraction method (*19*) and using ice from the more recent 5Γ Vostok core. A new detailed deuterium record with a resolution of 20 years or less has been measured (Fig. 1). It is in excellent agreement with published data (*1*) confirming, in particular, a two-step warming somewhat similar to what is observed for Termination I, with a return to colder conditions in the first part of the Termination. The $\delta^{40}Ar$ record (Fig. 1A) shows an increase of ~0.25‰ from 2815 to 2775 m (which occurs in two steps with a return to relatively low values around 2800 m). Such a $\delta^{40}Ar$ increase is indicative of an augmentation of the DCH by 11 m [or ~6 m if the part potentially resulting from thermal diffusion (*18*, *19*) is subtracted]. This result is surprising because firn densification models (*20*) predict that total firn thickness decreases in this depth interval. Similarly, the $\delta^{40}Ar$ decrease observed from 2775 to 2740 m corresponds to a depth interval over which the modeled total firn thickness increases (Figs. 1B and 2).

[1]Institut Pierre Simon Laplace/Laboratoire des Sciences du Climat et de l'Environnement, Commissariat à l'Energie Atomique/CNRS, L'Orme des Merisiers, CEA Saclay, 91191, Gif sur Yvette, France. [2]Scripps Institution of Oceanography, University of California San Diego, La Jolla, CA 92093–0244, USA. [3]Laboratoire de Glaciologie et Géophysique de l'Environnement, CNRS, BP96, 38402, Saint Martin d'Hères, France. [4]Polar Research Institute of China, Pudong, Shanghai, 200129, People's Republic of China. [5]Arctic and Antarctic Research Institute, Beringa Street 38, 199397 St. Petersburg, Russia.

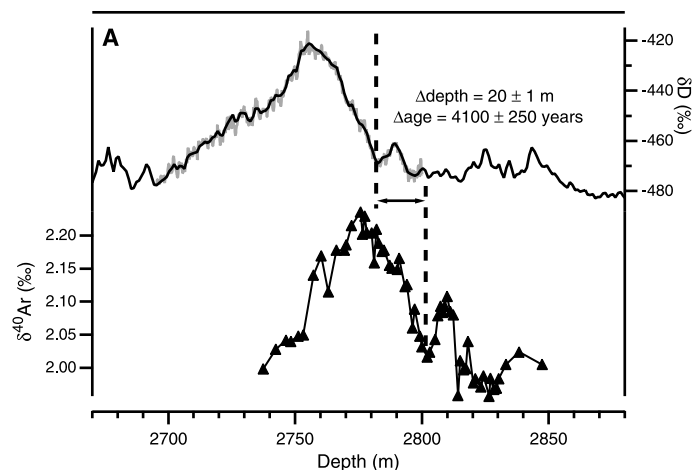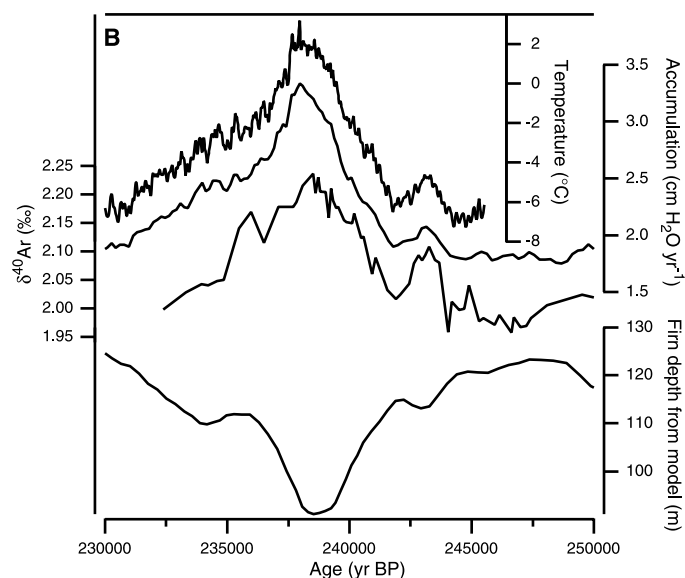*To whom correspondence should be addressed. E-mail: ncaillon@ucsd.edu

Fig. 1. (**A**) Vostok records covering Termination III with respect to depth. The deuterium measured in ice combines 1-m-resolution published data (*1*) (black curve) and a new set of detailed measurements (every 10 cm corresponding to a time resolution of ~20 years) performed between 2680 and 2800 m (gray curve). The δ⁴⁰Ar of gas trapped in air bubbles is shown (triangles) (duplicate measurements were carried out with a pooled standard deviation of 0.014‰). (**B**) Vostok records with respect to the GT4 time scale: temperature deduced from the deuterium record, the accumulation (*1*), the δ⁴⁰Ar profile, and the firn depth estimated using a firn densification model (*20*), whose result depends both on temperature and accumulation rate, with deeper firn depth for higher accumulation and colder temperatures. Temperature, accumulation, and δ⁴⁰Ar are very well correlated ($R^2 = 0.85$), which suggests that δ⁴⁰Ar may be used as a temperature proxy in the gas phase. The model firn depth and δ⁴⁰Ar data vary in antiphase during the warming.

The shapes of the δ⁴⁰Ar and deuterium records are remarkably similar, including the two-step shape mentioned above (Fig. 1B). Indeed, there is a strong positive correlation ($R^2 = 0.85$) between the δ⁴⁰Ar/DCH record and temperature and accumulation changes, which are both directly derived from the deuterium record (*21*). All three records are reported with respect to age using the GT4 time scale (*1*) both for the ice and the gas (*22*). The time scale in this interval may be in error due to uncertainty in the accumulation rates used in its construction. Because Vostok is not located on a dome, ice at depth originated upstream from Vostok in regions that today have higher accumulation than Vostok. This fact explains why the accumulation rates shown here (Fig. 1B) are higher than the present-day values at Vostok. As a result, accumulation is probably less well estimated at this site than it would be on a dome. Indeed, comparison of the Vostok and Dome Fuji isotope profiles suggests that Vostok accumulation is probably overestimated by 20% over the depth interval considered here (*23*).

Without time scale adjustment, the correlation between δ⁴⁰Ar and temperature (or accumulation, which in this case is directly derived from the temperature) gives $R^2 = 0.85$. Such a strong correlation would not likely be observed if the DCH thickness were not influenced by a change of either temperature or accumulation, or a combination of both. We favor the temperature interpretation based on the following qualitative arguments. First, the concurrent increase of DCH thickness and decrease of modeled total firn thickness during the deglaciation

Fig. 2. Plots versus depth in Vostok core: (i) the variation of the firn depth obtained using the firn densification model (*20*); (ii) the evolution of the DCH deduced from the δ⁴⁰Ar data and using the barometric equation (*17*). The isotopic composition of the air is related to the thickness of the diffusive column and to the ambient temperature through $\delta = [\exp(\Delta mgz/RT) - 1] \times 1000$, where Δm is the mass difference between isotopic species, z is the thickness of the diffusive column, g is the gravitational acceleration, R is the gas constant, and T is the firn temperature (in

kelvin), which is very close to the mean annual surface temperature at Vostok. The difference between total firn depth and DCH includes the convective plus nondiffusive zones (*17*). The negative firn depth around 2778 m is unphysical and can be explained by error in the total firn depth estimate.
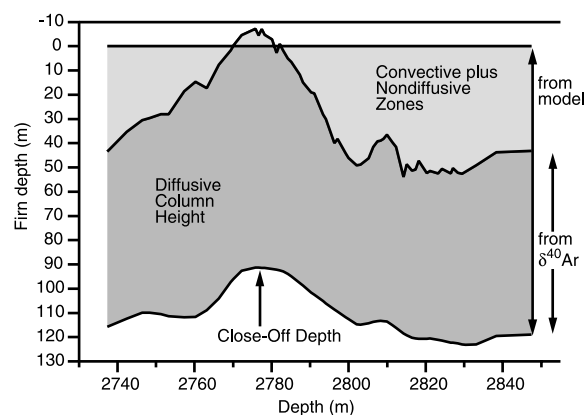
results in a disappearance of the calculated convective plus nondiffusive zones for the warmest part of the interglacial (Fig. 2). This disappearance is consistent with present (interglacial) field observations that find DCH equal to total firn thickness at most polar sites (*24–26*). Reduction in the thickness of convective and nondiffusive zones during Vostok interglacials has been previously reported (*17*). Second, climatically driven changes in the physical structure of the firn (such as layering or grain size) could enhance ventilation or increase the thickness of the nondiffusive zone during glacials. Third, the possibility that total firn thickness is well represented by DCH during glacials (and that the models are incorrect) cannot be ruled out, although we find this explanation unattractive

because it would violate time scale constraints (*1*, *25*). All of these options would explain the existence of a link between DCH thickness and temperature, but we cannot rule out accumulation as a contributing factor. DCH may be indirectly controlled by temperature, via accumulation, as accumulation is expected to vary positively with temperature (*21*). Further theoretical and field studies are necessary to decipher the processes involved. We will now proceed under the assumption that DCH is predominantly controlled by temperature, which provides, if correct, a signal of temperature change through a property measured in the gas phase. We first examine the sequence of events during Termination III as seen from properties measured in Vostok air bubbles, and then focus

on the phasing between CO_2 concentration change and Antarctic temperature.

Figure 3 compares profiles of δ^{40}Ar (assumed to be a proxy of Vostok temperature), CO_2, CH_4, and $\delta^{18}O_{atm}$, the isotopic composition of atmospheric oxygen. This figure is similar to that presented in (1), except that the use of a temperature proxy measured in air bubbles makes the comparison with other properties more accurate. The following conclusions are based on the assumption that there is no lag of δ^{40}Ar behind temperature (27) and so they must be considered tentative. We follow Petit et al. (1) in assuming that CH_4 can be used as a time marker of the glacial-interglacial warming in the

Northern Hemisphere. The CH_4 increase at 2810 m, which occurred when δ^{40}Ar reached its first maxima, would thus signal a first warming in the North leading to some equivalent of the Bølling-Allerød interval. We point here to the existence of a cold reversal at the start of Termination III (1), now firmly identified in both our detailed deuterium and δ^{40}Ar Vostok profiles. The sudden increase of 150 ppbv practically coeval with the δ^{40}Ar maximum would be linked to the main deglaciation, thus indicating that Vostok temperature began warming ~6000 years (Fig. 3) before the associated warming in the Northern Hemisphere (1). This interpretation is supported by the $\delta^{18}O_{atm}$ profile (28, 29),

but we recognize the difficulties of using this parameter as an indicator of the ice-volume changes associated with the deglaciation (29).

We confirm the close correlation between CO_2 and Vostok temperature during deglaciations (1). However, Fig. 3 indicates that CO_2 increases and peaks at a shallower depth in the core than δ^{40}Ar. To closely examine their phase relationship, we searched for the best fit between those two properties by adjusting the scaling ratio between δ^{40}Ar and CO_2. The best correlation ($R^2 = 0.88$) was obtained when we shifted the CO_2 profile by 800 ± 100 years (Fig. 4). Combining this uncertainty with the uncertainty introduced by ice accumulation (800 × 0.2, i.e., 160 years), we obtain an overall uncertainty of ±200 years, indicating that the increase in CO_2 lags Antarctic warming by 800 ± 200 years, which we must consider a mean phase lag because of the method we used to make the correlation. We cannot think of a mechanism that would make δ^{40}Ar lead the temperature change, although a lag is possible if the temperature or accumulation change affects the nondiffusive zone (27). This result is in accordance with recent studies (9, 30) but, owing to our new method, more precise. This confirms that CO_2 is not the forcing that initially drives the climatic system during a deglaciation. Rather, deglaciation is probably initiated by some insolation forcing (1, 31, 32), which influences first the temperature change in Antarctica (and possibly in part of the Southern Hemisphere) and then the CO_2. This sequence of events is still in full agreement with the idea that CO_2 plays, through its greenhouse effect, a key role in amplifying the initial orbital forcing. First, the 800-year time lag is short in comparison with the total duration of the temperature and CO_2 increases (~5000 years). Second, the CO_2 increase clearly precedes the Northern Hemisphere deglaciation (Fig. 3).

The similarity between CO_2 and Vostok temperature and the associated short time lag (30, 33) support the suggestion of Petit et al. (1) that CO_2 may be controlled in large part by the climate of the southern ocean. Although there is not yet clear support for this assertion (through models, for example), a delay of about 800 years seems to be a reasonable time period to transform an initial Antarctic temperature increase into a CO_2 atmospheric increase through oceanic processes. Indeed, it is not clear whether the link between the southern ocean climate and CO_2 is the result of a physical mechanism, such as a change in the vertical ocean mixing (34) or sea-ice cover changes (35), or a biological mechanism, such as atmospheric dust flux and ocean productivity (36, 37). The 800-year lag cannot really rule out any of these mechanisms as having sole control. Any of these mechanisms might plausibly require a finite amount of warming before CO_2 outgassing becomes significant. Nevertheless, we think that our results are more consistent with a process that involves

Fig. 3. Sequence of events surrounding Termination III obtained by comparing δ^{40}Ar data with CO_2, CH_4, and $\delta^{18}O_{atm}$ versus age. The CO_2 data (circles) combine published data (1, 44) and additional measurements performed at LGGE. The crosses indicate the CO_2 data obtained by Fischer et al. (30).
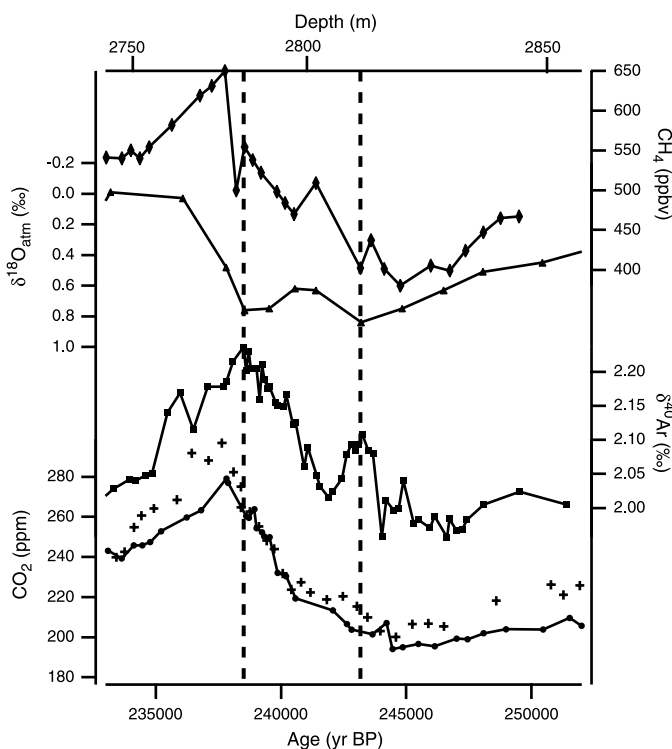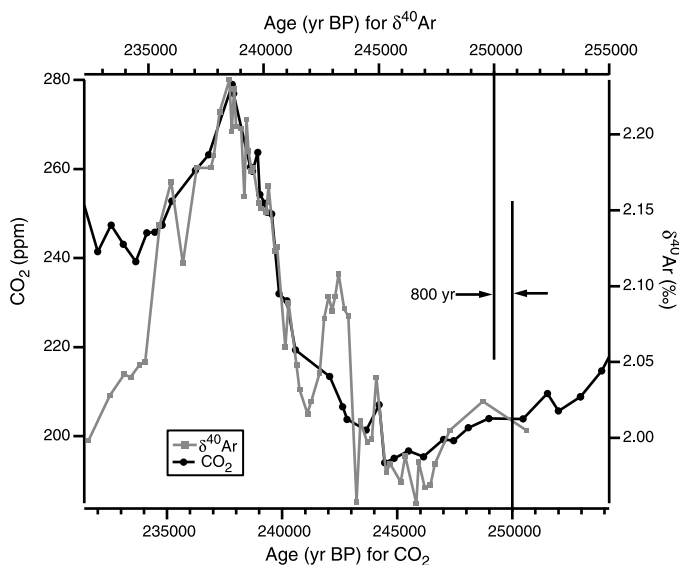

Fig. 4. Vostok records of δ^{40}Ar and CO_2 with respect to gas age (1). Atmospheric CO_2 concentration is a combination of new data and published data (1, 44). The age scale for the CO_2 proxy has been shifted by a constant 800 years to obtain the best correlation of the two datasets.

the deep ocean, as its mixing time is close to the observed 800-year lag.

Finally, the situation at Termination III differs from the recent anthropogenic CO_2 increase. As recently noted by Kump (*38*), we should distinguish between internal influences (such as the deglacial CO_2 increase) and external influences (such as the anthropogenic CO_2 increase) on the climate system. Although the recent CO_2 increase has clearly been imposed first, as a result of anthropogenic activities, it naturally takes, at Termination III, some time for CO_2 to outgas from the ocean once it starts to react to a climate change that is first felt in the atmosphere. The sequence of events during this Termination is fully consistent with CO_2 participating in the latter ~4200 years of the warming. The radiative forcing due to CO_2 may serve as an amplifier of initial orbital forcing, which is then further amplified by fast atmospheric feedbacks (*39*) that are also at work for the present-day and future climate.

References and Notes

1. J. R. Petit *et al.*, *Nature* **399**, 429 (1999).
2. A. Neftel, H. Oeschger, T. Staffelbach, B. Stauffer, *Nature* **331**, 609 (1988).
3. D. Raynaud *et al.*, *Science* **259**, 926 (1993).
4. J. M. Barnola, D. Raynaud, Y. S. Korotkevich, C. Lorius, *Nature* **329**, 408 (1987).
5. D. M. Sigman, E. A. Boyle, *Nature* **407**, 859 (2000).
6. In 1999, Fischer *et al.* (*30*) estimated that the increase of CO_2 lagged Vostok temperature by 600 ± 400 years at the start of the last three Terminations, but the gas age–ice age difference at Vostok may be uncertain by 1000 years (*1*) and thus obscures the phasing of gas variations with climate signals borne by the ice.
7. The firn is the uppermost part of an ice sheet. It can be schematically divided into three zones with different properties concerning the movement of air: the convective zone in which the air is well mixed, the diffusive zone in which vertical transport is driven by molecular diffusion, and the nondiffusive zone in which air does not migrate vertically, and at the bottom of which the air is trapped (*17*). This entrapped air is younger than the surrounding ice, which results in an age difference (Δage) between the ice and the air bubbles that it contains.
8. T. Blunier *et al.*, *Geophys. Res. Lett.* **24**, 2683 (1997).
9. E. Monnin *et al.*, *Science* **291**, 112 (2001).
10. N. Caillon, J. Jouzel, J. Chappellaz, A. Grachev, unpublished data.
11. C. Lang, M. Leuenberger, J. Schwander, S. Johnsen, *Science* **286**, 934 (1999).
12. M. Leuenberger, C. Lang, J. Schwander, *J. Geophys. Res.* **104**, 22163 (1999).
13. J. P. Severinghaus, T. Sowers, E. Brook, R. Alley, M. Bender, *Nature* **391**, 141 (1998).
14. J. P. Severinghaus, J. Brook, *Science* **286**, 930 (1999).
15. N. Caillon *et al.*, *J. Geophys. Res.* **106**, 31893 (2001).
16. The argon peak around 2760 m has no counterpart in the temperature record published in (*1*). In Fig. 1B, we plotted the temperature profile that we deduced from the new deuterium measurements performed every 10 cm (between 2700 and 2800 m). During the cooling phase of the interglacial, several abrupt temperature fluctuations occurred [especially around 235,000 years (2740 m)], which were not revealed by the temperature profile in (*1*). Those temperature variations could have affected the isotopic composition of argon, making the argon peak at 2760 m. However, the sampling frequency in this depth range (2775 to 2750 m) does not allow access to a δ^{40}Ar record as precise as that which we obtained during the Termination (i.e., between 2830 and 2775 m) and does not allow a peak-to-peak correlation.
17. T. A. Sowers, M. Bender, D. Raynaud, Y. S. Korotkevich, *J. Geophys. Res.* **97**, 15683 (1992).
18. Dynamic densification firn models accounting for heat transfer are now under development. First results predict that part of the measured argon signal should be a result of thermal diffusion (*40, 41*). Those models suggest that despite the slow time scale of warming during the Termination, there is still a small residual temperature gradient left over after thousands of years, because of the low thermal conductivity of the firn. The models generate a temperature gradient between surface and close-off region of about 3 K, which leads to a thermal diffusion signal of about 0.11‰ using measured thermal diffusion coefficients (*19, 42*). The use of a precise record of δ^{15}N, which is more sensitive to thermal diffusion than δ^{40}Ar/4, over the Termination should be useful to confirm the small thermal diffusion signal predicted by their models. Indeed, δ^{15}N data should have a slightly larger value than δ^{40}Ar/4 to be consistent with the presence of thermal diffusion signal (*13*). However, a precise record of δ^{15}N for Termination III is not available (fig. S1).
19. J. P. Severinghaus, A. Grachev, B. Luz, N. Caillon, *Geochim. Cosmochim. Acta* **67**, 325 (2003).
20. L. Arnaud, J.-M. Barnola, P. Duval, in *Physics of Ice Core Records*, T. Hondoh, Ed. (Hokkaido Univ. Press, Sapporo, Japan, 2000), pp. 285–305.
21. C. Lorius *et al.*, *Nature* **316**, 591 (1985).
22. The deuterium content of the snow in East Antarctica is linearly related to the surface temperature of the precipitation site. Jouzel and colleagues (*43*) have reviewed all relevant information focusing on the East Antarctic Plateau where both model and empirical isotope-temperature estimates are available. Combining arguments coming from the isotopic composition of the air bubbles, from constraints with respect to ice core chronologies, from atmospheric general circulation models, and from isotopic general circulation models (see references herein), the authors suggest that, unlike for Greenland, the present-day spatial isotope-temperature slope can be taken as a surrogate of the temporal slope to interpret glacial-interglacial isotopic changes at sites such as Vostok.
23. O. Watanabe *et al.*, *Nature*, in press.
24. J. P. Severinghaus, A. Grachev, M. Battle, *Geochem. Geophys. Geosyst.* **2**, Paper no. 2000GC000146 (2001).
25. N. Caillon, thesis, University of Paris 6, France (2001).
26. M. Battle *et al.*, *Nature* **383**, 231 (1996).
27. The nondiffusive zone is at the bottom of the firn and thus warms several hundred years after the surface because of the slow diffusion of heat through the firn (*4*). Additionally, the low accumulation rates at Vostok make the downward transport of firn physical properties rather slow (potentially spanning thousands of years). For example, if strong winds during the glacial periods created wind-packed layers that later impeded gas diffusion, thus creating a very thick nondiffusive zone, these layers would take several thousand years to be transported down to the nondiffusive zone.
28. T. Sowers, M. Bender, D. Raynaud, Y. S. Korotkevich, J. Orchado, *Paleoceanography* **6**, 669 (1991).
29. J. Jouzel *et al.*, *Quat. Sci. Rev.* **21**, 307 (2002).
30. H. Fischer, M. Wahlen, J. Smith, D. Mastroianni, B. Deck, *Science* **283**, 1712 (1999).
31. C. Genthon *et al.*, *Nature* **329**, 414 (1987).
32. N. J. Shackleton, *Science* **289**, 1897 (2000).
33. H. J. Smith, H. Fischer, M. Wahlen, D. Mastroianni, B. Deck, *Nature* **400**, 248 (1999).
34. J. R. Toggweiler, *Paleoceanography* **14**, 572 (1999).
35. B. Stephens, R. Keeling, *Nature* **404**, 171 (2000).
36. J. H. Martin, R. M. Gordon, S. E. Fitzwater, *Nature* **345**, 156 (1990).
37. W. S. Broecker, G. M. Henderson, *Paleoceanography* **13**, 352 (1998).
38. L. R. Kump, *Nature* **419**, 188 (2002).
39. C. Lorius, J. Jouzel, D. Raynaud, J. Hansen, H. Le Treut, *Nature* **347**, 139 (1990).
40. J. Schwander, personal communication.
41. C. Goujon, personal communication.
42. A. M. Grachev and J. P. Severinghaus, *Geochim. Cosmochim. Acta* **67**, 345 (2003).
43. J. Jouzel *et al.*, *J. Geophys. Res.*, in press.
44. L. Pépin, D. Raynaud, J.-M. Barnola, M. F. Loutre, *J. Geophys. Res.* **106**, 31885 (2001).
45. We acknowledge the effort of the Russian Antarctic expeditions (RAE), the division of Polar Programs (NSF), and the Institut Polaire Paul Emile Victor (IPEV) for their participation in the Vostok Project. We thank T. Sowers, M. Leuenberger, and J. Schwander for their pertinent and useful reviews; and J. Chappellaz, V. Masson-Delmotte, J.-R. Petit, F. Parrenin, H. Gildor, L. Pépin, M. Bender, R. Keeling, A. Landais, V. Caillon, C. Gougon, and B. Bellier for help and for fruitful comments and discussions. This work was supported by the French Programme National d'Études de la Dynamique du Climat (PNEDC), the CEA, the Balzam Foundation, the European program Pole-Ocean-Pole (POP EVK2-2000-00089), by NSF grants OPP 9725305 and ATM 9905241 (J.P.S.), and by recruitment funds from the Scripps Institution of Oceanography.

Climate and the Collapse of Maya Civilization

Gerald H. Haug,[1]*† Detlef Günther,[2] Larry C. Peterson,[3] Daniel M. Sigman,[4] Konrad A. Hughen,[5] Beat Aeschlimann[2]

In the anoxic Cariaco Basin of the southern Caribbean, the bulk titanium content of undisturbed sediment reflects variations in riverine input and the hydrological cycle over northern tropical South America. A seasonally resolved record of titanium shows that the collapse of Maya civilization in the Terminal Classic Period occurred during an extended regional dry period, punctuated by more intense multiyear droughts centered at approximately 810, 860, and 910 A.D. These new data suggest that a century-scale decline in rainfall put a general strain on resources in the region, which was then exacerbated by abrupt drought events, contributing to the social stresses that led to the Maya demise.

Paleoclimatologists have developed an increasingly precise record of climate change for the past few millennia, covering the same span of time over which literate human societies developed. Until recently, archaeologists and historians have lacked information about short-term climate change during the period of human societal evolution, being forced into the assumption that global climate has been nearly invariant for at least the past 6000 years. How-